Communication-Aware Robotics: Exploiting Motion for Communication

Arjun Muralidharan, and Yasamin Mostofi

Department of Electrical and Computer Engineering, University of California Santa Barbara, Santa Barbara, 93106; email: arjunm@ece.ucsb.edu, ymostofi@ece.ucsb.edu

. :1–27

Keywords

communication-aware path planning, exploiting mobility for connectivity, real channel environments, probabilistic channel prediction, co-optimization of motion and communication, first passage distance, minimum-energy operation, robotic routers, robotic beamformers

Abstract

In this review, we present a comprehensive perspective on the area of communication-aware robotics, where realistic communication environments are considered and communication and navigation issues are jointly optimized. Theoretical characterization and understanding performance guarantees will be the main focus of this article. We start by summarizing the best prediction an unmanned vehicle can have of the channel quality at unvisited locations. We then consider the case of a single robot and see how it can mathematically characterize the statistics of its traveled distance until connectivity, and further plan its path to reach a connected spot with optimality guarantees, in real channel environments and with minimum energy consumption. We then move to the case of multiple robots and see how they can utilize their motions to enable robust information flow. We consider two specific robotic network configurations: robotic beamformers and robotic routers and mathematically characterize properties of the co-optimum motion-communication decisions.

Contents

1. INTRODUCTION

Over the past few decades there has been an unprecedented growth in sensing, communication, computation, and actuation, driving a revolution in sensor networks and robotics. Teams of autonomous robots, each equipped with sensing and communication capabilities, can sense and interact with their environment, and cooperatively work towards achieving a common goal. Such robotic networks are envisioned to play an increasingly important role in a wide range of tasks such as emergency response, surveillance, service provisioning, agriculture, data gathering, and extending cellular network coverage.

Wireless communication plays an integral role in robotic network operations as unmanned vehicles need to connect to other nodes or to a remote operator, for instance to transfer sensing data and/or to receive control commands. Maintaining connectivity and ensuring a robust flow of information is thus a fundamental problem that arises in robotic networks. Since each robot's path directly affects its link quality, each unmanned vehicle needs to take the communication quality into account when path planning.

This area of research where a group of unmanned vehicles explicitly take communication link qualities into account when path planning is known as *communication-aware robotics*. In communication-aware robotics, each node explicitly assesses the impact of its motion decisions on its link quality and co-optimizes its communication, navigation, and sensing objectives. This results in interesting interplays between the optimum motion, communication, and sensing parameters as these parameters are now coupled in the decision making process. Considering the underlying energy constraints, in terms of both communication and navigation, further creates interesting interplays between the communication and motion decisions.

Figure 1 shows sample scenarios of networked robotic operations. Communication-aware robotics is the main topic of this review, with a special focus on utilizing the motion of the robots to enable/optimize connectivity, and co-design the underlying communication and navigation objectives.

Figure 1: Sample robotic operations (best viewed in color): (top-left) search and rescue, (top-right) mobile service provisioning, (bottom-left) extending coverage of cellular systems, and (bottom-right) optimizing connectivity of home networks. Background image courtesy of (top-left) US Navy, (top-right) Getty Images, and (bottom row) PixalBay.

1.1. State Of The Art

The idea of multi-robot systems began in the 1980s (e.g., seminal work of (1)), followed by much more extensive work in the following decades on a wide range of applications. Due to the already-complex nature of multi-robot operations in terms of path planning, distributed decision making, and sensing, earlier work in multi-robot systems did not consider communication issues. In the past decade, however, the importance of jointly considering communication objectives along with motion and sensing goals has been recognized. For instance, the impact of communication has been considered in several networked robotic tasks such as coverage control (2–4), field sensing (5, 6), search and surveillance (7–11), target tracking (12), flocking (13–15), consensus (16, 17), SLAM (18, 19), task allocation and servicing (20–23), and robotic routing protocols (24, 25).

In more recent years, a new set of applications have also emerged where unmanned vehicles are envisioned to be used to extend the connectivity of cellular systems or indoor home/office router networks, examples of which are shown in **Figure 1 (bottom row)**. This has resulted in a broad range of recent work on using the mobility of robotic systems to enable and optimize communication. For instance, robot mobility can be exploited for point-to-point communication (26–32), relaying (33–41), beamforming (42–46), data gathering (47–54), and communication coverage (55, 56).

Historically, earlier work in communication-aware robotics utilized over-simplified models of connectivity, such as disk models or path-loss only models (7, 11, 34, 36, 48), due to the already-complex nature of the underlying multi-robot problem. Such models, however, cannot properly capture the spatial variations of wireless links in real environments (e.g., see sample channel measurement of **Figure 2 (right)**). Thus, control strategies built on such over-simplified models can experience significant performance degradation when im-

plemented in practice. More recent work has utilized more realistic channel models. For instance, in (57, 58), a probabilistic channel prediction framework is introduced, by considering the three major underlying dynamics of the channel, which allows the robots to estimate a probability density function (PDF) of the channel quality at unvisited locations, based on a small number of a priori or online channel samples. This probabilistic framework has since been utilized by a number of robotic work (4, 8, 12, 28, 31, 35, 38, 44, 45, 47, 50, 59–67) and has interesting implications for robotic path planning and networked robotic operations.

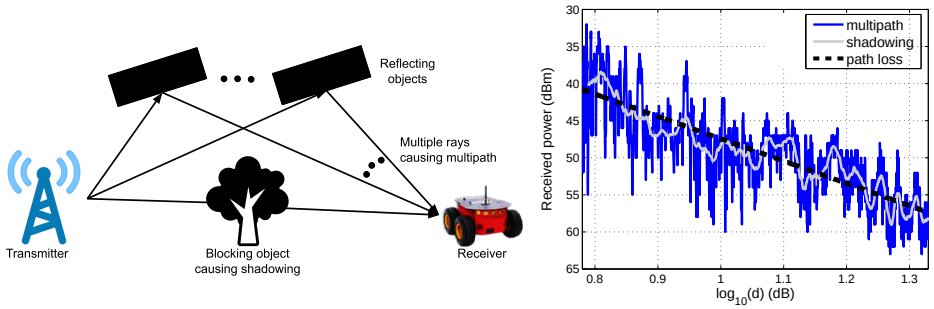

Figure 2: (left) A toy environment that illustrates the channel components. (right) A sample received power along an indoor route together with its underlying dynamics: path loss, shadowing, and multipath. Figure adapted from (58).

It is our goal in this review to present a comprehensive perspective on communication-aware robotics and the corresponding co-optimization of communication and navigation in realistic channel environments, with an emphasis on theoretical characterization and understanding performance guarantees.

1.2. Review Outline

In Section 2, we review a realistic channel model that utilizes the main three dynamics of wireless links: path loss, shadowing and multipath. We then proceed with mathematically characterizing the best prediction an unmanned vehicle can have of the channel quality at unvisited locations, based on a small number of online or a priori channel samples. As we shall see, the best prediction is a probabilistic estimate that builds a PDF for the channel at an unvisited location, using the aforementioned three underlying dynamics.

We then begin with the case of a single robot in Sections 3 and 4, with the goal of presenting a mathematical understanding of optimum communication-aware robotic decisions. Here, we see how an unmanned vehicle can mathematically characterize the statistics of its distance traveled until connectivity, and further plan its path to reach a guaranteed connected spot, with minimum energy consumption, and while achieving an asymptotic ϵ-suboptimal solution.

In Section 5, we then move to the case of multiple robots utilizing their motions to enable robust information flow and connectivity. We consider two specific robotic network configurations: robotic beamformers and robotic routers. Our focus here is to understand and mathematically characterize properties of the co-optimum motion-communication decisions and the interplay between the two. In Section 6, we then briefly mention other aspects of communication-aware robotics. Finally, we summarize the key findings and dis-

cuss potential future directions.

2. CHANNEL MODELING AND PREDICTION

Traditionally, ideal communication links or disk models have been heavily utilized in the robotics literature in order to spatially model a communication link at unvisited locations, for the purpose of path planning. In a disk model, there is perfect connectivity within a certain radius of a transmitting node, with no connection outside of it. A disk model, however, is a poor representation of the link quality. **Figure 2 (right)**, for instance, shows a real channel measurement (58). As can be seen, the link is far from ideal, and a disk model would be a poor representation of the link. In more recent years, it has been acknowledged that a better prediction of the link quality is needed for the purpose of robotic field operation, and that consequently a more multi-disciplinary approach that jointly considers both communication and navigation issues is needed. Along this line, new methods have been developed, based on empirical channel models, that aim to probabilistically predict the channel power at unvisited locations, based on a number of online or a priori channel samples in the area. In this section, we review this realistic probabilistic modeling of the spatial variations of a wireless channel, and the subsequent prediction framework that allows the robots to probabilistically predict the channel at unvisited locations (57, 58). This probabilistic framework has been utilized by a number of robotic work in recent years (4, 8, 12, 28, 31, 35, 38, 44, 45, 47, 50, 59–67).

2.1. Probabilistic Channel Modeling

In the communication literature, a wireless channel is well modeled as a random process with three main spatial dynamics: (a) a slowly-varying (with respect to space) path loss component that accounts for decay in the channel power with distance, (b) a faster-varying shadowing component (also called large-scale fading) that accounts for attenuation effects of buildings, trees and other large obstructing structures, and (c) an even faster-varying multipath component (also called small-scale fading) that accounts for scattering and reflection (68). **Figure 2 (right)** shows a sample received channel power along an indoor route together with its constituent dynamics.

Let $\Gamma(q_1)$ denote the received channel power (in dB) at location $q_1 \subset \mathbb{R}^2$ due to a transmitting station located at $q_b \in \mathbb{R}^2$. Then

$$\Gamma(q_1) = \gamma_{\rm PL}(q_1) + \Gamma_{\rm SH}(q1) + \Gamma_{\rm MP}(q1), \qquad 1.$$

where $\gamma_{\rm PL}(q_1) = K_{\rm dB} - 10n_{\rm PL}\log_{10}\|q_1 - q_b\|$ is the path loss component with $n_{\rm PL}$ denoting the path loss coefficient. $\Gamma_{\rm SH}(q_1)$ is the shadowing component and is best modeled as a zero-mean Gaussian random process with an exponentially-decaying correlation function: $\mathbf{E}[\Gamma_{\rm SH}(q_1)\Gamma_{\rm SH}(q_2)] = \sigma^2_{\rm SH}e^{-\|q_1-q_2\|/\beta_{\rm SH}}$ with $\sigma^2_{\rm SH}$ representing the shadowing power and $\beta_{\rm SH}$ denoting the decorrelation distance (68). Finally $\Gamma_{\rm MP}(q_1)$ is the multipath component, and is also best modeled as a random process with a number of distributions such as Nakagami, Rician, and lognormal found to be good fits for its distribution (68, 69).

2.2. Probabilistic Channel Prediction

We next see how an unmanned vehicle can use the previous empirical channel modeling in order to probabilistically predict the channel power at unvisited locations (i.e., predict the

corresponding PDFs), based on a number of online or a priori channel samples in the area (57, 58).

Let $\Gamma_q = [\Gamma_{q_1}, \cdots, \Gamma_{q_m}]^{\mathrm{T}}$ denote the vector of m collected channel measurements at locations $q = [q_1, \cdots, q_m]^{\mathrm{T}}$ in the workspace of interest. These small number of measurements can be collected by the robot before the operation. Alternatively, they can be collected by other robots in past operations and stored in the cloud. The robot can also use the channel measurements it collects during the operation to predict the channel at unvisited locations in an online manner.

The following theorem (58) shows how the robot can estimate the channel at unvisited locations based on a small number of prior samples.

Theorem 1 *A Gaussian random vector $\Gamma(r) = [\Gamma(r_1), \cdots, \Gamma(r_k)]^{\mathrm{T}} \sim \mathcal{N}(\overline{\Gamma}(r), \Sigma(r))$ can best characterize the channel power (in dB) at unvisited locations $r = [r_1 \cdots r_k]^{\mathrm{T}}$, with the mean and covariance matrix given by*

$$\overline{\Gamma}(r) = G_r\hat{\vartheta} + \Xi_{r,q}\left(\Xi_q + \hat{\sigma}^2_{MP} I_m\right)^{-1}\left(\Gamma_q - G_q\hat{\vartheta}\right), \tag{2.}$$

$$\Sigma(r) = \Xi_r + \hat{\sigma}^2_{MP} I_k - \Xi_{r,q}\left(\Xi_q + \hat{\sigma}^2_{MP} I_m\right)^{-1}\Xi^{\mathrm{T}}_{r,q}, \tag{3.}$$

respectively, where $G_r = [\mathbf{1}_k \ -L_r]$, $G_q = [\mathbf{1}_m \ -L_q]$, $\mathbf{1}_m$ ($\mathbf{1}_k$) represents the m-dimensional (k - dimensional) vector of all ones, I_m (I_k) represents the m-dimensional (k - dimensional) identity matrix, $L_q = \left[10\log_{10}(\|q_1 - q_b\|) \ \cdots \ 10\log_{10}(\|q_m - q_b\|)\right]^{\mathrm{T}}$, $L_r = \left[10\log_{10}(\|r_1 - q_b\|) \ \cdots \ 10\log_{10}(\|r_k - q_b\|)\right]^{\mathrm{T}}$ and q_b is the position of the remote station. Furthermore, Ξ_q, Ξ_r and $\Xi_{r,q}$ denote matrices with entries $\left[\Xi_q\right]_{i_1,i_2} = \hat{\sigma}^2_{SH} e^{-\|q_{i_1} - q_{i_2}\|/\hat{\beta}_{SH}}$, $\left[\Xi_r\right]_{j_1,j_2} = \hat{\sigma}^2_{SH} e^{-\|r_{j_1} - r_{j_2}\|/\hat{\beta}_{SH}}$, $\left[\Xi_{r,q}\right]_{j_1,i_1} = \hat{\sigma}^2_{SH} e^{-\|r_{j_1} - q_{i_1}\|/\hat{\beta}_{SH}}$ respectively, where $i_1, i_2 \in \{1, \cdots, m\}$, and $j_1, j_2 \in \{1, \cdots, k\}$. Moreover, $\vartheta = [K_{\mathrm{dB}} - n_{\mathrm{PL}}]^{\mathrm{T}}$, β_{SH}, σ^2_{SH} and σ^2_{MP} denote the path loss parameters, the decorrelation distance of shadowing, the power of shadowing (in dB) and the power of multipath (in dB) respectively. The $\hat{}$ symbol denotes the estimate of the corresponding parameter.

The underlying channel parameters can be estimated from a few a priori measurements as well. For more details see (58). Using this framework, the robot can then predict a PDF for the channel at unvisited locations of the workspace for the purposes of path planning. **Figure 3** shows a sample 2D channel and its predicted mean from Theorem 1 using 5% prior channel samples in the space. Note that the predicted variance at each unvisited location can then serve as the corresponding uncertainty in channel learning.

We next start with one robot and see how it can mathematically characterize and optimize its connectivity before moving to a network of unmanned vehicles.

3. DISTANCE TRAVELED UNTIL CONNECTIVITY

Consider the scenario where a robot is seeking to establish connection with a remote node as it moves along a pre-defined path as shown in **Figure 4**. One important factor that the robot may need to assess is its distance until connectivity, i.e., how much longer it needs to travel before it gets connected, as it can play a key role in its field decision making. We next characterize how the robot can mathematically characterize the PDF of its distance until connectivity (28) using the probabilistic channel model of Section 2.

Establishing connectivity requires that a certain Quality of Service such as a minimum

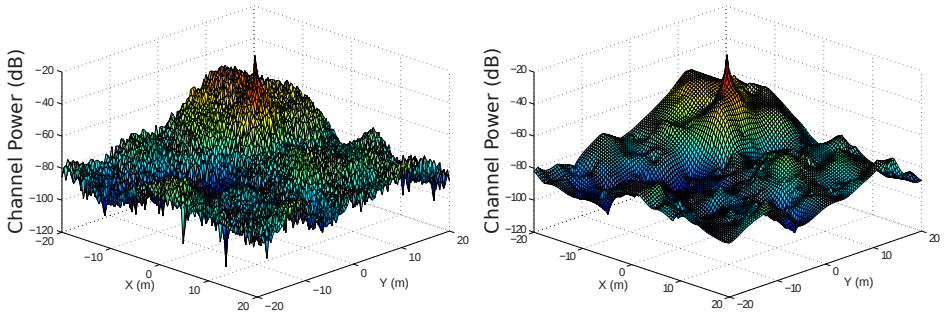

Figure 3: (right) The mean of the estimated channel power based on a small number of randomly-distributed prior measurements (5%) of the (left) true channel map in a 2 dimensional workspace.

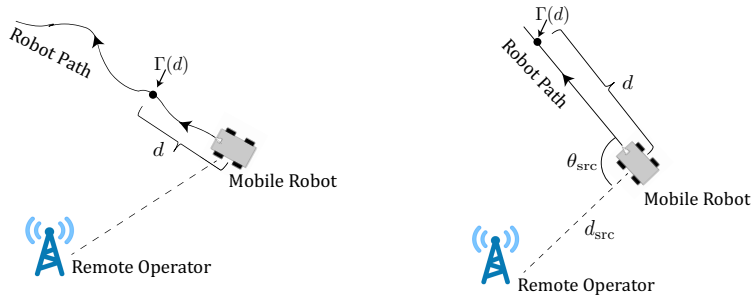

Figure 4: What is the distance traveled by the robot before it finds a connected spot along (left) a general path and (right) a straight path? Figure adapted from (28).

bit error rate be satisfied, which in turn, translates to a minimum required channel power, which we shall denote by γ_{th}. A location q is thus said to be connected if $\Gamma(q) \geq \gamma_{\text{th}}$.

With a slight abuse of notation, for the remainder of this section, let $\Gamma(d) = \gamma_{\text{PL}}(d) + \Gamma_{\text{SH}}(d) + \Gamma_{\text{MP}}(d)$ denote the channel power at a distance d along the given path. We are then interested in characterizing the distance traveled by the robot until it finds a connected spot. In (32), this distance is referred to as the first passage distance (FPD) drawing a parallel with the concept of first passage time.[1] We next see how to mathematically characterize the PDF of the ϵ-upcrossing FPD, which is the FPD given that the robot is initially disconnected. More specifically, the random variable $\mathcal{D}^{\epsilon}_{\Gamma_0} = \inf_{d>0}\{d : \Gamma(d) \geq \gamma_{\text{th}} | \Gamma(0) < \gamma_{\text{th}} - \epsilon\}$ denotes the ϵ-upcrossing FPD, where $\Gamma(0)$ is a random variable upper bounded by $\gamma_{\text{th}} - \epsilon$.[2] Consider the complementary cumulative dis-

[1]First passage time is the time until a random process first hits a threshold (70) and has extensively been used in diverse fields such as brownian motion modeling, neuronal firing characterization, and stock market analysis.

[2]We require that $\epsilon > 0$ since the mathematical tools used are not well defined for $\epsilon = 0$. However, ϵ can be considered arbitrarily small.

GAUSS-MARKOV PROCESS

Gaussian Process

A stochastic process $\{X(t) : t \in \mathcal{T}\}$, where $\mathcal{T}$ is an index set, is a Gaussian process, if any finite number of samples have a joint Gaussian distribution, i.e., $(X(t_1), X(t_2), \cdots, X(t_k))$ is a Gaussian random vector for all $t_1, \cdots, t_k \in \mathcal{T}$ and for any k (71).

A Gaussian process is completely specified by its mean function $m_X(t) = \mathbb{E}[X(t)]$ and its covariance function $\Sigma_X(t_1, t_2) = \mathbb{E}\{[X(t_1) - m_X(t_1)][X(t_2) - m_X(t_2)]\}$. We use the notation $X \sim \mathcal{GP}(m_X, \Sigma_X)$ to denote the underlying process.

Markov Process

A process $X(t)$ is a Markov process if $\Pr\big(X(t_n) \leq x_n | X(t_{n-1}), \cdots, X(t_1)\big) = \Pr\big(X(t_n) \leq x_n | X(t_{n-1})\big)$, for all n and for all $t_n \geq t_{n-1} \geq \cdots \geq t_1$, where $\Pr(.)$ denotes the probability of the argument (72).

Gauss-Markov Process

A stochastic process is Gauss-Markov if it satisfies the requirements of both a Gaussian process and a Markov process (73).

Connected location: $q_1 \in \mathbb{R}^2$ is said to be connected if the received channel power at q_1 is greater than the minimum required channel power, i.e., $\Gamma(q_1) \geq \gamma_{\text{th}}$.

First passage distance (FPD): The distance traveled by the robot along a path until a connection is established.

tribution function (CCDF) of $\mathcal{D}^{\epsilon}_{\Gamma_0}$: $\Pr\left(\mathcal{D}^{\epsilon}_{\Gamma_0} > d\right) = \Pr\big(\Gamma(b) < \gamma_{\text{th}}, \forall b < d | \Gamma(0) < \gamma_{\text{th}} - \epsilon\big)$, which is what the robot is interested in evaluating. A direct naive computation of this would involve a high-dimensional prohibitive integration over the probabilistic Gaussian channel model of Section 2. In other words, assuming we discretize the path into N steps and the domain of $\Gamma(d)$ into M parts, this would have a computational complexity of $O(NM^N)$, which quickly becomes infeasible for even moderate values of N and M. We next see how the robot can mathematically evaluate its FPD in a way that is both theoretically meaningful and computationally efficient, i.e., $O(N^2)$ when multipath is negligible and $O(NM\log(M))$ otherwise.

We start by considering the statistics of the FPD for a straight path, followed by a characterization of the FPD for a more general space of paths.

3.1. First Passage Distance (FPD) For A Straight Path

Consider a robot starting from an initial distance of d_{src} from the remote station, and traveling along a straight path in the direction specified by θ_{src}, as shown in **Figure 4**. The path loss component $\gamma_{\text{PL}}(d)$ is then expressed as $\gamma_{\text{PL}}(d) = K_{\text{dB}} - 5n_{\text{PL}}\log_{10}(d^2_{\text{src}} + d^2 - 2d_{\text{src}}d\cos\theta_{\text{src}})$.

We first consider the case where multipath is negligible, followed by a more general analysis with multipath included.

3.1.1. Case of Negligible Multipath: Stochastic Differential Analysis. Characterization of FPD while ignoring multipath effects is directly applicable to cases where multipath is negligible due to a low number of scatterers or when we want to find a small area of good

connectivity as opposed to a single well-connected spot. Moreover, this analysis further gives us insight into the general FPD characterization.

For negligible multipath, we are then interested in when $\Gamma(d) = \gamma_{\rm PL}(d) + \Gamma_{\rm SH}(d)$ is greater than $\gamma_{\rm th}$. As summarized in the following Lemma (28), $\Gamma_{\rm SH}(d)$ and subsequently $\Gamma(d)$ can be shown to be Gauss-Markov processes (see the sidebar on Gauss-Markov processes).

Lemma 1 *The channel shadowing power $\Gamma_{SH}(d)$ and subsequently the channel power $\Gamma(d)$ are Gauss Markov processes with characterization $\mathcal{GP}(0, \Sigma_{SH})$ and $\mathcal{GP}(\gamma_{PL}, \Sigma_{SH})$ respectively, where $\Sigma_{SH}(b, d) = \sigma^2_{SH} e^{-(d-b)/\beta_{SH}}$.*

In fact, $\Gamma_{\rm SH} \sim \mathcal{GP}(0, \Sigma_{\rm SH})$ is the famous Ornstein-Uhlenbeck process, one of the most well-studied Gauss-Markov processes (74).

Using the Gauss-Markov literature (75), the transition PDF $f(\gamma, d|\eta, b)$ characterizing the distribution of $\Gamma(d)$ given $\Gamma(b) = \eta$ can be found to satisfy the partial differential equation known as the Fokker-Plank equation, as follows (28)

$$\frac{\partial}{\partial d} f(\gamma, d|\eta, b) = -\frac{\partial}{\partial \gamma} \left[A_{\rm FP}(\gamma, d) f(\gamma, d|\eta, b) \right] + \frac{1}{2} \frac{\partial^2}{\partial \gamma^2} \left[B_{\rm FP} f(\gamma, d|\eta, b) \right], \qquad 4.$$

with the associated initial condition of $f(\gamma, b|\eta, b) = \delta(\gamma - \eta)$, where $A_{\rm FP}(\gamma, d) = \gamma'_{\rm PL}(d) - (\gamma - \gamma_{\rm PL}(d))/\beta_{\rm SH}$, $B_{\rm FP} = (2\sigma^2_{\rm SH})/\beta_{\rm SH}$, $\gamma_{\rm PL}(d)$ is the path loss component, and $\gamma'_{\rm PL}(d)$ is its derivative.

The channel power $\Gamma(d)$ can also be represented as a stochastic differential equation,

$$\mathrm{d}\Gamma(d) = A_{\rm FP}(\Gamma, d)\mathrm{d}d + \sqrt{B_{\rm FP}}\mathrm{d}\overline{W}(d), \qquad 5.$$

where $\overline{W}(d)$ represents the Wiener process and $A_{\rm FP}(\gamma, d)$ and $B_{\rm FP}$ are as defined before.

Remark 1 *$A_{FP}(\gamma, d)$ and B_{FP} are known as the drift and diffusion components respectively. More specifically, in an increment Δd, we can think of the channel power spatially evolving with a deterministic rate of $A_{FP}(\gamma, d)$, while a zero-mean random Gaussian term with the variance of $B\Delta d$ is superposed on it.*

The following result builds on the Fokker-Plank equation and provides a recursive integral equation to find the PDF of the ϵ-upcrossing FPD (28).

Theorem 2 *Let $g_u^{(\epsilon)}[d]$ denote the PDF of the ϵ-upcrossing FPD. $g_u^{(\epsilon)}[d]$ satisfies the following non-singular second-kind Volterra integral equation:*

$$g_u^{(\epsilon)}[d] = -2\Psi_u^{(\epsilon)}[d] + 2\int_0^d g_u^{(\epsilon)}[b]\Psi[d|\gamma_{th}, b]\mathrm{d}b, \qquad 6.$$

where $\Psi[d|\eta, b] = \left\{ -\frac{1}{2}\frac{\mathrm{d}\gamma_{PL}(d)}{\mathrm{d}d} - \frac{\gamma_{th}-\gamma_{PL}(d)}{2\beta_{SH}} \frac{1+e^{-2(d-b)/\beta_{SH}}}{1-e^{-2(d-b)/\beta_{SH}}} + \frac{\eta-\gamma_{PL}(b)}{\beta_{SH}} \frac{e^{-(d-b)/\beta_{SH}}}{1-e^{-2(d-b)/\beta_{SH}}} \right\} f(\gamma_{th}, d|\eta, b)$, $\Psi_u^{(\epsilon)}[d] = \frac{1}{2\Pr(\Gamma(0)<\gamma_{th}-\epsilon)} \left\{ \frac{-2\sigma^2_{SH}}{\beta_{SH}} e^{-d/\beta_{SH}} f(\gamma_{th} - \epsilon, 0) f[\gamma_{th}, d|\gamma_{th} - \epsilon, 0] + \frac{1}{2} f(\gamma_{th}, d)(1 + \mathrm{Erf}[\Upsilon_\epsilon(d)]) \left(-\frac{\mathrm{d}\gamma_{PL}(d)}{\mathrm{d}d} - \frac{1}{\beta_{SH}} [\gamma_{th} - \gamma_{PL}(d)] \right) \right\}$, *with* $\mathrm{Erf}(z) = \frac{2}{\sqrt{\pi}} \int_0^z e^{-t^2} \mathrm{d}t$ *representing the error function, and* $\Upsilon_\epsilon(d) = \frac{\gamma_{th}-\epsilon-\gamma_{PL}(0)-e^{-d/\beta_{SH}}(\gamma_{th}-\gamma_{PL}(d))}{\sqrt{2\sigma^2_{SH}\left(1-e^{-2d/\beta_{SH}}\right)}}$.

This enables the robot to mathematically characterize the PDF of its distance until connectivity. Furthermore, the recursive integral of Theorem 2 serves as the basis for an efficient iterative algorithm (using Simpson's rule) to compute the PDF of the FPD in $O(N^2)$ (see (75) for details).

3.1.2. Including Multipath Effects: A Recursive Characterization. In this section, we consider the more general channel model of $\Gamma(d) = \gamma_{\mathrm{PL}}(d) + \Gamma_{\mathrm{SH}}(d) + \Gamma_{\mathrm{MP}}(d)$. The results of Section 3.1.1 are not applicable anymore since the overall channel power $\Gamma(d)$ is not a Gauss-Markov process once we include the multipath component in our analysis. However, the shadowing power $\Gamma_{\mathrm{SH}}(d)$ is still a Markov process, and we can use this to obtain a methodology to compute the PDF of the FPD recursively. Let us assume that the robot measures the channel along the straight path in discrete steps of size Δd. We further assume that the multipath component is uncorrelated at two points separated by Δd, which is a reasonable assumption since the multipath component typically decorrelates fast (58). We then index the channel power based on the steps taken, i.e., let $\Gamma_k = \Gamma(k\Delta d)$ and $\Gamma_{\mathrm{SH},k} = \Gamma_{\mathrm{SH}}(k\Delta d)$.

We are then interested in the characterization of the FPD $\mathcal{K} = \min_{1,2,\cdots}\{k : \Gamma_k \geq \gamma_{\mathrm{th}}, \Gamma_0 < \gamma_{\mathrm{th}}\}$. This can be expressed in terms of its CCDF as

$$\Pr(\mathcal{K} = k) = \Pr(\mathcal{K} > k-1) - \Pr(\mathcal{K} > k). \tag{7.}$$

Note that this CCDF probability can be expressed as

$$\Pr(\mathcal{K} > k) = \Pr\big(\Gamma_1, \cdots, \Gamma_k < \gamma_{\mathrm{th}} | \Gamma_0 < \gamma_{\mathrm{th}}\big) = \frac{\int_{\gamma_{\mathrm{SH},k}=-\infty}^{\infty} \Omega_k(\gamma_{\mathrm{SH},k}) \mathrm{d}\gamma_{\mathrm{SH},k}}{\Pr(\Gamma_0 < \gamma_{\mathrm{th}})}, \tag{8.}$$

where

$$\Omega_k(\gamma_{\mathrm{SH},k}) = \int_{\gamma_{\mathrm{MP},k}=-\infty}^{\gamma_{\mathrm{th}}-\gamma_{\mathrm{PL}}(d_k)-\gamma_{\mathrm{SH},k}} \int_{S_{k-1}} \cdots \int p(\gamma_{\mathrm{SH},0}, \gamma_{\mathrm{MP},0}, \cdots, \gamma_{\mathrm{SH},k}, \gamma_{\mathrm{MP},k}) \times \mathrm{d}\gamma_{\mathrm{SH},0}\mathrm{d}\gamma_{\mathrm{MP},0} \cdots \mathrm{d}\gamma_{\mathrm{SH},k-1}\mathrm{d}\gamma_{\mathrm{MP},k-1}\mathrm{d}\gamma_{\mathrm{MP},k} \tag{9.}$$

with $S_{k-1} = \cap_{i=0}^{k-1}\{\gamma_{\mathrm{SH},i}, \gamma_{\mathrm{MP},i} : \gamma_{\mathrm{PL}}(d_i) + \gamma_{\mathrm{SH},i} + \gamma_{\mathrm{MP},i} < \gamma_{\mathrm{th}}\}$ and $p(\gamma_{\mathrm{SH},0}, \gamma_{\mathrm{MP},0}, \cdots, \gamma_{\mathrm{SH},k}, \gamma_{\mathrm{MP},k})$ representing the joint probability density of $\Gamma_{\mathrm{SH},0}, \Gamma_{\mathrm{MP},0}, \cdots, \Gamma_{\mathrm{SH},k}$, and $\Gamma_{\mathrm{MP},k}$.

We can compute the functions $\Omega_k(\gamma_{\mathrm{SH},k})$ recursively as shown in the following lemma (28).

Lemma 2 *The functions Ω_k of Equation 9, for $k = 1, \cdots, N$, can be computed by the recursion:*

$$\Omega_{k+1}(\gamma_{SH,k+1}) = F_{MP}\big(\gamma_{th} - \gamma_{PL}(d_{k+1}) - \gamma_{SH,k+1}\big)\frac{1}{\varrho}\int_{u=-\infty}^{\infty} \varphi\left(\frac{\gamma_{SH,k+1} - u}{\sigma_{SH}\sqrt{1-\varrho}}\right)\Omega_k\left(\frac{u}{\varrho}\right)\mathrm{d}u, \tag{10.}$$

initialized with $\Omega_0(\gamma_{SH,0}) = F_{MP}\big(\gamma_{th} - \gamma_{PL}(0) - \gamma_{SH,0}\big)\varphi\left(\frac{\gamma_{SH,0}}{\sigma_{SH}}\right)$, where $F_{MP}(.)$ is the CDF of the multipath random variable Γ_{MP} and $\varphi(.)$ is the standard Gaussian density function.

We can then use Lemma 2 to calculate the PDF of the FPD efficiently using Equations 7 and 8.

KULLBACK-LIEBLER DIVERGENCE

The KL divergence between two distributions $p(x)$ and $\tilde{p}(x)$ is defined as

$$KL = \int p(x) \log_e \frac{p(x)}{\tilde{p}(x)} dx.$$

KL divergence is a measure of the distance between two distributions (76). We utilize the KL divergence as a measure of how close to Markovian the channel shadowing power along a general path is.

3.2. First Passage Distance (FPD) For A General Path

The results of the previous section was for a straight path and utilized the fact that the shadowing power $\Gamma_{\text{SH}}(d)$ is a Gauss-Markov Process on a straight path. The channel shadowing power along a general non-straight path, however, may not be a Gauss-Markov process. Still, we can characterize a large set of paths for which the shadowing power is approximately Markovian, and use the results of the previous section to characterize the FPD.

Consider a point at a distance d along a general path as shown in **Figure 4 (left)**. The shadowing power at this point and at the point a step behind (for a step size of Δd) are given by $\Gamma_{\text{SH}}(d)$ and $\Gamma_{\text{SH}}(d-\Delta d)$ respectively. The FPD characterization of Section 3.1 followed from the Markovian nature of the shadowing power, i.e., $p\big(\gamma_{\text{SH}}(d)|\gamma_{\text{SH}}(d-\Delta d), \{\gamma_{\text{SH}}(d-b), \forall b > \Delta d\}\big) = p\big(\gamma_{\text{SH}}(d)|\gamma_{\text{SH}}(d-\Delta d)\big)$. Thus, a path is approximately-Markovian if at every point on the path, these two distributions are close. We use the Kullback-Liebler divergence (see sidebar on KL divergence) between the distributions as a measure of how close they are. The smaller the KL divergence the closer the path is to Markovian, and the more applicable the characterization of the FPD of Section 3.1 will be. However, mathematically characterizing the KL divergence between these two distributions can be intractable. Instead, we consider the pairwise KL divergences between $p\big(\gamma_{\text{SH}}(d)|\gamma_{\text{SH}}(d-\Delta d), \gamma_{\text{SH}}(d-b)\big)$ and $p\big(\gamma_{\text{SH}}(d)|\gamma_{\text{SH}}(d-\Delta d)\big)$ for all $b > \Delta d$, and for all d. If these pairwise KL divergences are small enough, we declare the path to be approximately-Markovian. The KL divergence between the distributions of $\Gamma_{\text{SH}}(d)|\Gamma_{\text{SH}}(d-\Delta d), \Gamma_{\text{SH}}(d-b)$ and $\Gamma_{\text{SH}}(d)|\Gamma_{\text{SH}}(d-\Delta d)$, for a $b > \Delta d$, is a Chi-squared random variable (77). We then formally define an approximately-Markovian path as follows (see (28)).

Definition 1 (Approximately-Markovian Path) *Let $m_{KL}(d,b)$ and $\sigma_{KL}(d,b)$ denote the mean and standard deviation of the KL divergence between $p\big(\gamma_{SH}(d)|\gamma_{SH}(d-\Delta d), \gamma_{SH}(d-b)\big)$ and $p\big(\gamma_{SH}(d)|\gamma_{SH}(d-\Delta d)\big)$ for a given $b > \Delta d$. A path is approximately-Markovian for parameters ϵ_m and ϵ_σ if $m_{KL}(d,b) \leq \epsilon_m$ and $\sigma_{KL}(d,b) \leq \epsilon_\sigma$, for all $b > \Delta d$ and for all d.*

We can determine if a path is approximately-Markovian, for parameters ϵ_m and ϵ_σ, based purely on properties of the path (e.g., its curvature), and the underlying channel parameters (e.g., decorrelation distance). The intuition here is that if the curvature of the path is small enough, and if the path does not loop around, then the path can be considered approximately-Markovian. The following theorem (28) formalizes this intuition and precisely characterizes sufficient conditions for an approximately-Markovian path.

Theorem 3 (Approximately-Markovian Path) *Let $r(d) = (x(d), y(d))$ be a path parameterized by its arc length. The path is approximately-Markovian for given maximum tolerable KL divergence parameters ϵ_m and ϵ_σ, if it satisfies the following conditions:*

1. $\|r(d) - r(d-b)\| > d_{th}$, *for* $b > \frac{1}{\kappa}\sin^{-1}(\kappa d_{th})$ *and for all* d,
2. *curvature* $\kappa(d) < \kappa_{th}$ *for all* d,

where $d_{th} = \frac{\beta_{SH}}{2}\log_e\left(\varrho^2 + \frac{1-\varrho^2}{\epsilon_d}\right)$, *and* κ_{th} *is obtained by solving the following optimization problem*

$$\begin{aligned} &\textit{maximize} && \kappa \\ &\textit{subject to} && \max_{\phi:0<\phi\leq\psi_{cons}(\kappa)} \psi_{opt}(\kappa,\phi) \leq \epsilon_d \\ & && \kappa < 1/d_{th}, \end{aligned} \tag{11.}$$

where $\psi_{opt}(\kappa,\phi) = \dfrac{\left(e^{-\frac{2}{\kappa\beta_{SH}}\sin\left(\frac{\phi+\Delta\phi}{2}\right)} - \varrho e^{-\frac{2}{\kappa\beta_{SH}}\sin\left(\frac{\phi}{2}\right)}\right)^2}{\left(1-e^{-\frac{4}{\kappa\beta_{SH}}\sin\left(\frac{\phi}{2}\right)}\right)(1-\varrho^2)}$, $\psi_{cons}(\kappa) = 2\sin^{-1}\left(\frac{\kappa d_{th}}{2}\right) - \Delta\phi$, $\Delta\phi = 2\sin^{-1}\left(\frac{\kappa\Delta d}{2}\right)$, $\varrho = e^{-\Delta d/\beta_{SH}}$, *and* $\epsilon_d = \min\left\{1 - e^{-2\epsilon_m}, \sqrt{2}\epsilon_\sigma\right\}$.

Note that several general paths satisfy the conditions of Theorem 3, as shown in (28). For instance, **Figure 5 (left)** shows an archimedian spiral path, which can be confirmed to be approximately Markovian. **Figure 5 (right)** further shows the CDF of the ϵ-upcrossing FPD for this path using Lemma 2. We can see that the theoretical derivations are a good match to the true statistics obtained via Monte Carlo simulations. The underlying channel was generated with parameters obtained from real channel measurements in downtown San Francisco (78).

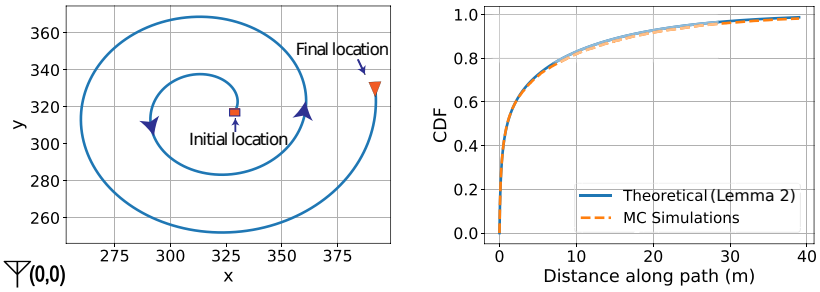

Figure 5: (left) Archimedian spiral as the path of the robot, and (right) the CDF of upcrossing FPD when including multipath using Lemma 2. Figure adapted from (28).

The results of this section show how an unmanned vehicle can theoretically characterize the statistics of its distance traveled until connectivity in a mathematical framework that is also computationally very efficient.

4. PATH PLANNING TO ESTABLISH CONNECTIVITY

In this section, we consider the case where the robot can also plan its path such that it minimizes the *expected traveled distance* until it finds a *guaranteed connected* spot to a remote station (30, 31). The robot, operating in a realistic channel environment experiencing path

loss, shadowing, and multipath fading, has an estimate of the connectivity across space using the channel prediction framework of Section 2. The robot can then plan its path exploiting this channel prediction such that it minimizes the expected traveled distance until it gets connected (see **Figure 6 (left)**). As we shall see, this problem can be solved with asymptotic optimality guarantees in a graph-theoretic setting (31).

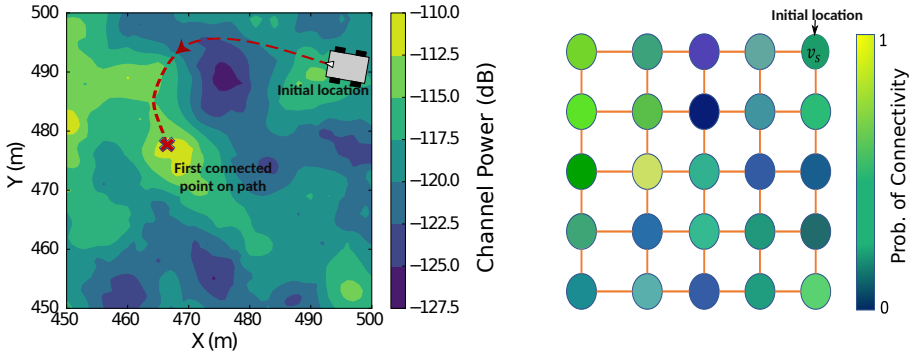

Figure 6: A robot plans its path such that it minimizes the expected distance until it gets connected to a remote station, in a realistic channel environment that experiences path loss, shadowing, and multipath fading. (left) The workspace of the robot with the background representing the mean of the predicted channel quality, and (right) the graph-theoretic representation of the workspace where every node is associated with a probability of connectivity derived from the predicted channel quality. Figure (left) is adapted from (30).

Let us discretize the workspace of the robot into cells to form a grid graph $\mathcal{G} = (\mathcal{V}, \mathcal{E})$, with each cell serving as a node in the graph. Each node $v \in \mathcal{V}$ is associated with a probability of connectivity $p_v \in [0, 1]$, and each edge $(u, v) \in \mathcal{E}$ is associated with a length $l_{u,v} > 0$ representing the distance between two nodes u and v in the workspace. A cell is connected if there exists a location in the cell that is connected. For instance, consider a cell/node v that consists of positions $r = [r_1, \cdots, r_k]^T$. The probability of connectivity of cell v is then given by $p_v = 1 - \Pr\big(\Gamma(r_i) < \gamma_{\text{th}}, \forall i \leq k\big)$, where $\Gamma(r) = [\Gamma(r_1) \cdots \Gamma(r_k)]^{\text{T}} \sim \mathcal{N}\left(\overline{\Gamma}(r), \Sigma(r)\right)$ is a Gaussian random vector obtained from the channel prediction framework of Section 2, and γ_{th} is the minimum required channel power for connectivity. For the mathematical analysis of this section, we assume that the probability of connectivity at a node is independent of the connectivity at any other node in the workspace.

The objective is to then generate a path, starting from a node $v_s \in \mathcal{V}$, that *minimizes the expected traveled distance until connectivity*. Note that the robot may only traverse part of the generated path, as its planning is based on a probabilistic channel characterization and it may get connected at any node along the path. For the expected traveled distance until connectivity to be well defined for a path, the probability of failure after traversing the entire path must be zero, implying that the final node must be a node where $p_v = 1$. We call such a node a terminal node and define $T = \{v \in \mathcal{V} : p_v = 1\}$. For instance, the remote station can serve as a terminal node. The expected cost of a path $\mathcal{P} = (v_1, v_2, \cdots, v_m = v_t)$ can then be expressed as $C(\mathcal{P}) = \sum_{e \in \mathcal{E}(\mathcal{P})} \left[\prod_{v \in \mathcal{V}(\mathcal{P}_e)} (1 - p_v)\right] l_e$, where $\mathcal{E}(\mathcal{P})$ denotes the set of edges belonging to the path $\mathcal{P}$, and $\mathcal{V}(\mathcal{P}_e)$ denotes the set of vertices encountered along

GAME THEORY PRIMER

A game $\{\mathcal{V}', \{A_v\}, \{\mathcal{J}_v\}\}$, consists of the following components: 1) the players (agents) of the game: $\mathcal{V}'$, 2) the action set of player v: A_v, and 3) the local cost function of player v: $\mathcal{J}_v : A \to \mathbb{R}$, where $A = \prod_{u \in \mathcal{V}'} A_u$.

Nash Equilibrium. An action profile μ^{NE} is said to be a pure Nash equilibrium if $\mathcal{J}_v(\mu^{\text{NE}}) \leq \mathcal{J}_v(\mu_v, \mu^{\text{NE}}_{-v}),\ \forall \mu_v \in A_v, \forall v \in \mathcal{V}'$ where μ_{-v} denotes the action profile of all players except v (79).

Potential Game. $\{\mathcal{V}', \{A_v\}, \{\mathcal{J}_v\}\}$ is a potential game over action space $A_S \subset A$ if there exists a function $\Phi : A_S \to \mathbb{R}$, such that $\mathcal{J}_v(\mu_v', \mu_{-v}) - \mathcal{J}_v(\mu_v, \mu_{-v}) = \Phi(\mu_v', \mu_{-v}) - \Phi(\mu_v, \mu_{-v})$, for all $\mu = (\mu_v, \mu_{-v}) \in A_S$, $v \in \mathcal{V}'$, and μ_v' such that $(\mu_v', \mu_{-v}) \in A_S$, where μ_{-v} denotes the action profile of all players except v (31, 80).

Min-Exp-Dist-Path Problem: The optimization problem to find the path that minimizes the expected traveled distance until connectivity.

$\mathcal{P}$ until the edge $e \in \mathcal{E}(\mathcal{P})$. Note that the robot estimates the probability of connectivities (p_vs) using the probabilistic prediction framework of Section 2. The optimization problem of interest, to which we refer as the **Min-Exp-Dist-Path** problem, can then be posed as (31)

$$\begin{aligned} \underset{\mathcal{P}}{\text{minimize}} \quad & C(\mathcal{P}) = \sum_{e \in \mathcal{E}(\mathcal{P})} \left[\prod_{v \in \mathcal{V}(\mathcal{P}_e)} (1 - p_v) \right] l_e \\ \text{subject to} \quad & \mathcal{P} \text{ is a path of } \mathcal{G} \text{ such that } \mathcal{P}[1] = v_s, \mathcal{P}[\text{end}] \in T. \end{aligned} \tag{12.}$$

Theorem 4 *The Min-Exp-Dist-Path problem of Equation 12 is an NP-hard problem.*

The proof is based on showing that the decision version of the problem is NP-complete, using a reduction to a rooted version of the NP-complete Hamiltonian path problem (31).

We next see how an ϵ-suboptimal solution to Equation 12 can be achieved by posing this problem in a game-theoretic setting. Note that, in what follows, the robot is using game theory solely to design its own path and as such can make all the decisions locally.

4.1. Game-Theoretic Communication-Aware Path Planner

Consider a game $\{\mathcal{V}', \{A_v\}, \{\mathcal{J}_v\}\}$ where the set of non-terminal nodes $\mathcal{V}' = \mathcal{V}/\mathcal{T}$ of the previously-defined graph are the players of the game, and the action set $A_v = \{u \in \mathcal{V} : (u, v) \in \mathcal{E}\}$ is the set of neighbors of node v. Let $\mu_v \in A_v$ be the action of player/node v and let μ be the joint action profile.

We first describe the path produced from a node v and its expected distance until connectivity in terms of the action profile μ. An action profile μ induces a directed graph, $\mathcal{SG}(\mu)$, on $\mathcal{G}$, which has directed edges from v to μ_v. A node u is said to be *upstream* of v in $\mathcal{SG}(\mu)$ if v lies on the directed path from u to the corresponding sink. We denote the set of upstream nodes of v as $U_v(\mu_{-v})$ and let $v \in U_v(\mu_{-v})$ by definition. Let $\mathcal{P}(\mu, v)$ be the directed path from node v on $\mathcal{SG}(\mu)$, and let $C_v(\mu) = C(\mathcal{P}(\mu, v))$ denote the expected cost from node v when following the path $\mathcal{P}(\mu, v)$. Let A_{ASG} denote the set of action profiles such that the expected cost $C_v(\mu) < \infty$ for all $v \in \mathcal{V}$. This will only happen if the path $\mathcal{P}(\mu, v)$ ends at a terminal node for all v. This corresponds to $\mathcal{SG}(\mu)$ being

a directed acyclic graph with terminal nodes as sinks. Then $\mu \in A_{\text{ASG}}$ implies that the action of player v belongs to the constrained action set $A_v^c(\mu_{-v})$, i.e., $\mu_v \in A_v^c(\mu_{-v})$, where $A_v^c(\mu_{-v}) = \{u \in \mathcal{V} : (v,u) \in \mathcal{E}, u \notin U_v(\mu_{-v}), C_u(\mu) < \infty\}$ is the set of actions that result in a finite expected cost from v.

Upstream node: A node u is said to be upstream of v in the directed graph $\mathcal{SG}(\mu)$ if v lies on the directed path from u to the corresponding sink.

Next, consider local cost functions $\mathcal{J}_v$ of the form

$$\mathcal{J}_v(\mu) = \sum_{u \in U_v(\mu)} \varsigma_u C_u(\mu), \tag{13.}$$

where $U_v(\mu)$ is the set of upstream nodes of v, and $\varsigma_u > 0$ are constants such that $\varsigma_{v_s} = 1$ and $\varsigma_v = \epsilon^{'}$, for all $v \neq v_s$, where $\epsilon^{'} > 0$ is a small constant.

Then, these local cost functions result in a potential game over A_{ASG} as summarized in the next lemma (see (31) for the proof).

Lemma 3 *The game $\{\mathcal{V}', \{A_v\}, \{\mathcal{J}_v\}\}$, with local cost functions as defined in Equation 13, is a potential game over A_{ASG} with a potential function*

$$\Phi(\mu) = \sum_{v \in \mathcal{V}'} \varsigma_v C_v(\mu) = C_{v_s}(\mu) + \epsilon^{'} \sum_{v \neq v_s} C_v(\mu). \tag{14.}$$

4.1.1. Asymptotically ϵ-suboptimal Path Planner. We shall next see how to asymptotically obtain the global minimizer of $\Phi(\mu)$, and thereby find an ϵ-suboptimal solution to the Min-Exp-Dist-Path problem of Equation 12, by utilizing a learning process known as log-linear learning (31, 81).

Consider a potential game over the following complete graph. The complete graph $\mathcal{G}_{\text{comp}}$ is formed from $\mathcal{G}$ by adding an edge between all nodes that don't share an edge. The length of an added edge (u,v) is set to be the shortest distance between u and v. Then, the log-linear process operating on this potential game with constrained action sets $A_v^c(\mu_{-v}(k))$ asymptotically reaches an ϵ-suboptimal solution to the Min-Exp-Dist-Path problem, as formally summarized below (31).

Theorem 5 *Consider the Min-Exp-Dist-Path problem of Equation 12. Consider log-linear learning on a potential game over the complete graph $\mathcal{G}_{comp}$ with local cost functions as defined in Equation 13, and $\epsilon' = \epsilon / (|\mathcal{V}'|D)$, where D is the diameter of the graph. Then, as the temperature τ associated with log-linear learning goes to zero, i.e., $\tau \to 0$, the process asymptotically provides an ϵ-suboptimal solution to the Min-Exp-Dist-Path problem.*

4.1.2. Fast Non-Myopic Path Planner. Log-linear learning provides an ϵ-suboptimal solution to the Min-Exp-Dist-Path problem asymptotically. However, in certain scenarios, finding a suboptimal but fast solution may be more important.

The best reply process (79) operating on the potential game of Lemma 3 with constrained action sets $A_v^c(\mu_{-v}(k))$ converges to a pure Nash equilibrium, which is also a directionally local minimum of $\Phi(\mu) = C_{v_s}(\mu) + \epsilon^{'} \sum_{v \neq v_s} C_v(\mu)$ (see (31) for more details). The best reply process converges quickly to a directionally local minimum (e.g., after at most $|\mathcal{V}'|$ iterations (31)), and is thus an efficient path planner.

Figure 7 shows the histogram of the distance traveled until connectivity for a robot for the best reply path planner as well as a heuristic approach of moving straight towards the remote station, which we use as a benchmark. The histogram is over 500 channel realizations, where the underlying channel is generated using real channel parameters from

downtown San Francisco (78), and where the traveled distance is calculated based on the true channel quality. We can see that the distance associated with the best reply planner is much smaller than that associated with the benchmark. Log-linear learning performs the same or better than the best reply approach at a larger computation cost.

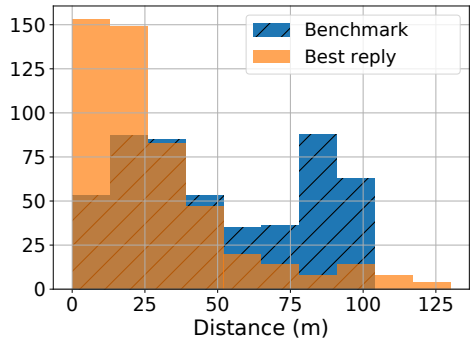

Figure 7: Histogram of the traveled distance for the best reply approach of Section 4.1.2 and a benchmark (where the robot moves straight towards the remote station) over 500 channel realizations. Figure adapted from (31).

Overall, this section showed how an unmanned vehicle can optimize its path to get to a connected spot, in realistic channel environments and with minimum energy consumption. As we saw, by using probabilistic channel prediction and a game-theoretic inspired path planning approach, it was possible to find an asymptotic ϵ-suboptimal global solution to this problem as well as fast solutions that can achieve a Nash Equilibrium.

5. MULTI-ROBOT NETWORK CONNECTIVITY

In Sections 3 and 4, we considered the scenario of a single robot utilizing its motion to enable and optimize its connectivity with a remote station under energy constraints. In this section, we consider the case where multiple robots exploit their motion to cooperatively enable and optimize connectivity in realistic communication environments. Depending on the task at hand, a team of unmanned vehicles may need to form different network configurations to enable the needed connectivity and information flow. For instance, a particular task may need the nodes to keep a fully-connected network throughout the operation, while another task may require a less-connected network or may allow the nodes to get disconnected from the team momentarily. While the nodes can in principle utilize their mobility to realize any given network configuration with a desired level of connectivity, here we focus on two particular network configurations, robotic beamformers and robotic routers, which can enable connectivity in otherwise poorly-connected areas.

Robotic Beamforming: In robotic beamforming, unmanned vehicles can cooperatively generate a strong link in an otherwise poorly-connected environment.

5.1. Cooperative Robotic Beamforming

Consider the scenario shown in **Figure 8**, where a team of unmanned vehicles, located in a poorly-connected area, want to exploit their mobility to cooperatively generate a strong link to a remote station, to which we refer as cooperative robotic beamforming.

In traditional transmit beamforming, a number of co-located antennas align their transmission phases such that the wireless signals constructively merge at the remote station, providing dramatic gains in the received signal power (82). In distributed beamforming, this is extended to several fixed nodes distributed across space, which emulates a virtual antenna array (83, 84). In effect, transmit beamforming allows nodes to cooperatively generate a strong link with dramatic signal to noise ratio (SNR) gains. The existing literature (83, 84) also describes how to effectively deal with timing and phase synchronization issues to produce the constructive interference required for beamforming in a distributed setting. Reference (85) further shows how to do beamforming with only signal magnitude, which can be useful if phase synchronization is not possible.

We can then extend the same concept to a team of unmanned vehicles and further utilize their mobility to move to locations better for distributed transmit beamforming. Consider the scenario shown in **Figure 8** where a team of unmanned vehicles need to establish connectivity to a remote node. However, the link quality for establishing individual communication is not strong enough in the area. The unmanned vehicles can then utilize their mobility to move to locations that are best for forming a virtual distributed antenna array for transmit beamforming. Such robotic beamforming networks have been a subject of recent studies (42–46). We next pose the underlying communication and motion co-optimization problem in real channel environments and discuss how an ϵ-suboptimal solution can be achieved (45).

Figure 8: Distributed robotic transmit beamforming: Multiple robots cooperatively generate a strong communication link to the remote station by optimizing their locations. Figure adapted from (45).

Consider a case where N_r robots are in a poorly-connected area with r_i denoting the position of robot i. As discussed in Sections 3 and 4, in order to successfully get connected to the remote station, a minimum received channel power, γ_{th}, needs to be satisfied. The received channel power (in the linear domain) at the remote station, after cooperative transmit beamforming by the N_r robots, is given by $\left(\sum_{i=1}^{N_r} \alpha(r_i)\rho_i\right)^2$ where $\alpha(r_i) = 10^{\Gamma(r_i)/20}$ is the channel amplitude when transmitting from location r_i, and $\rho_i \in [0, 1]$ is the fraction of the maximum allowable transmit power used by robot i. Note that $\Gamma(r_i)$ denotes the received channel power in dB when transmitting from location r_i. Let r and ρ denote the vector of the robot locations and the transmission coefficients respectively. The connectivity constraint on the overall beamformed signal can then be expressed as $\sum_{i=1}^{N_r} \alpha(r_i)\rho_i \geq \sqrt{\gamma_{\text{th,lin}}}$ where $\gamma_{\text{th,lin}} = 10^{\gamma_{\text{th}}/10}$ is the minimum required channel power in the linear domain. The robots can utilize the channel prediction framework of Section 2 to obtain a conservative estimate of the channel amplitude $\tilde{\alpha}(r_i)$ at an unvisited location r_i,

such that $20\log_{10}\tilde{\alpha}(r_i) = \overline{\Gamma}(r_i) - \zeta\sigma(r_i)$ for some constant $\zeta \geq 0$, where $\mathcal{N}(\overline{\Gamma}(r_i), \sigma(r_i)^2)$ is the predicted channel power distribution (in dB), when transmitting from r_i, obtained from Theorem 1.

The optimization problem to successfully connect to the remote station, while minimizing the total energy consumption, can then be expressed as follows (45), where the unmanned vehicles have to co-optimize their motion variables (r) and communication transmit power (ρ).

$$\begin{aligned} \underset{r_i,\rho_i}{\text{minimize}} \quad & K_M \sum_{i=1}^{N_r} \|r_i - r_i^0\| + \frac{n_{\text{bits}}}{\mathcal{R}(r,\rho)} P_0 \sum_{i=1}^{N_r} \rho_i^2 \\ \text{subject to} \quad & \sum_i \tilde{\alpha}(r_i)\rho_i \geq \sqrt{\gamma_{\text{th,lin}}} \\ & 0 \leq \rho_i \leq 1,\ i = 1, \cdots, N_r, \end{aligned} \tag{15.}$$

where $K_M \sum_{i=1}^{N_r} \|r_i - r_i^0\|$ is the total motion energy consumed to move to final locations r_is from initial locations r_i^0s, with K_M denoting the motion energy coefficient, and $\frac{n_{\text{bits}}}{\mathcal{R}(r,\rho)} P_0 \sum_{i=1}^{N_r} \rho_i^2$ is the communication energy needed to transmit n_{bits} of information at rate $\mathcal{R}(r,\rho) = \pi_1 W \log_2\left(1 + \pi_2 P_0 \frac{\left(\sum_{i=1}^{N_r} \tilde{\alpha}(r_i)\rho_i\right)^2}{N_0}\right)$ where W, N_0, and P_0 represent the bandwidth, the noise power, and the maximum transmit power of a robot respectively, and π_1, π_2 are constants depending on the communication scheme.

Theorem 6 *The ϵ-suboptimal solution (final locations r and transmission coefficients ρ) to the optimization problem of Equation 15 can be found by solving $O\left(N_r/\epsilon\right)$ multiple choice knapsack problems.*

See (45) for the proof and more details on the multiple choice knapsack problems. Theorem 6 shows that the robotic beamforming problem can be solved in realistic communication environments with performance guarantees.

We refer the interested readers to (45) for simulation results on robotic beamforming in realistic communication environments using Equation 15, which illustrates the benefits of motion and communication co-optimization.

5.2. Robotic Router Formation

An interesting problem in communication-aware robotics is that of robotic router formation for optimizing connectivity. There has been a considerable interest in this problem in recent years (33–35, 39, 86, 87). Consider the case where two remote field nodes need to communicate but are too far from each other. A number of unmanned vehicles can act as mobile routers and move to positions optimum for routing the information between the remote nodes, as illustrated in **Figure 9**. In earlier work, graph-theoretic approaches were utilized to optimize connectivity of a mobile relay network, without considering realistic communication channels or the end-to-end performance metrics, while more recent work has considered co-optimization of communication and motion parameters in realistic channel environments. We next start by discussing graph-theoretic approaches to solve this problem followed by considering the true cost of communication and co-optimizing motion and communication parameters.

5.2.1. A Graph-Theoretic Approach to Robotic Routers. The Fielder eigenvalue is a measure of how connected a graph is, and can be used as a measure of the connectivity within

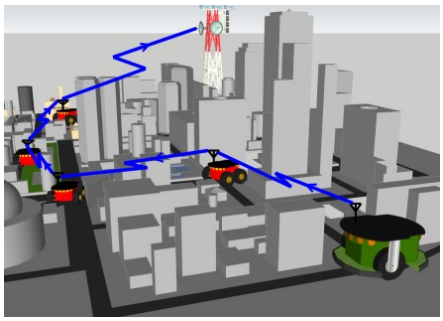

Figure 9: Robotic router formation – Multiple robots need to move to positions best for acting as relays between two remote nodes that are too far to directly establish connectivity.

a robotic network (39, 86), or between two remote nodes (33). Thus, one possible solution to the robotic router position optimization problem is to have the unmanned vehicles form a graph that has a high Fielder eigenvalue. Consider the state-dependent graph $\mathcal{G} = (\mathcal{V}, \mathcal{E})$ denoting the network of mobile robots where the set of vertices $\mathcal{V} = \{1, \cdots, N_r\}$ is the set of N_r nodes, with the first and last nodes indicating the fixed remote nodes and the rest denoting the $N_r - 2$ robots. Let $r = [r_1, \cdots, r_{N_r}]^T$ denote the location of the nodes. An edge between robots i and j in the graph is modeled in (33) as a distance-dependent weight $w(r_i, r_j) = f_{\text{conn}}(\|r_i - r_j\|)$ that uses a disk model, as follows: f_{conn} is 1 when the distance between robots i and j is less than a threshold, and rapidly drops to 0 as the distance increases beyond the threshold (39). The weighted graph Laplacian matrix $\mathcal{L}_\mathcal{G}(r)$ is given by the entries $[\mathcal{L}_\mathcal{G}(r)]_{ij} = \begin{cases} -w(r_i, r_j), & \text{if } i \neq j \\ \sum_{i \neq k} w(r_i, r_k), & \text{if } i = j \end{cases}$.

We then have the following optimization problem to maximize the Fielder eigenvalue of the robotic network (33)

$$\underset{r_i}{\text{maximize}} \quad \lambda_2 \left(\mathcal{L}_\mathcal{G}(r)\right) \tag{16.}$$

where $\lambda_2 \left(L_\mathcal{G}(r)\right)$ denotes the second smallest eigenvalue of the Laplacian matrix (also known as the Fielder value). Equation 16 can be solved using semi-definite programming (39) or via a decentralized algorithm using super-gradient (86).

In this Fielder value formulation, however, realistic channel models are not taken into account and an over-simplified disk model is assumed. Furthermore, the true performance of a robotic router can be best characterized by how accurately it relays the transmitted bits between the two remote nodes. The next part then poses a motion and communication co-optimization problem that takes these considerations into account.

5.2.2. Robotic Router Formation In Realistic Channel Environments. Using the probabilistic channel prediction framework of Theorem 1, the channel power between the $(i-1)^{\text{th}}$ and i^{th} robots, $\Gamma(r_{i-1}, r_i)$, can be best modeled as a Gaussian random variable with mean $\overline{\Gamma}(r_{i-1}, r_i)$ and standard deviation $\sigma(r_{i-1}, r_i)$. We can then pose the following optimization problem to maximize the probability of correct bit reception between the end nodes, for an

M_s-QAM communication scheme (35),

$$\begin{aligned} \underset{r_i}{\text{maximize}} \quad & \mathbb{E}\left\{\prod_{i=2}^{N_r}\left(1-0.2\exp\left\{-\frac{1.5P_0}{(M_s-1)N_0}10^{\frac{\Gamma(r_{i-1},r_i)}{10}}\right\}\right)\right\} \\ \text{subject to} \quad & r_i \in \mathcal{W},\ \ i=2,\cdots,N_r-1 \end{aligned} \tag{17.}$$

where N_r is the total number of nodes with the first and last nodes indicating the fixed remote nodes and N_r-2 robots in between. r_i is then the location of the i^{th} robot, $\mathcal{W}\subseteq\mathbb{R}^2$ is the workspace of the robots, P_0 is the transmit power, N_0 is the noise power, and $\Gamma(r_{i-1},r_i)$ is the random variable denoting the estimate of the channel between the $(i-1)^{\text{th}}$ and i^{th} nodes.

This optimization problem can be well approximated as follows (see (35) for details),

$$\underset{r_i}{\text{maximize}} \quad \sum_{i=2}^{N_r}\ln\left(1-0.2\left(1+\frac{1.5P_0}{(M_s-1)N_0}\xi(r_{i-1},r_i)10^{\frac{\overline{\Gamma}(r_{i-1},r_i)}{10}}\right)^{-\iota(r_{i-1},r_i)}\right), \tag{18.}$$

where $\iota(r_{i-1},r_i) = \left(\exp\left\{(a\sigma(r_{i-1},r_i))^2\right\}-1\right)^{-1}$ and $\xi(r_{i-1},r_i) = \exp\left\{1.5\left(a\sigma(r_{i-1},r_i)\right)^2\right\}-\exp\left\{0.5\left(a\sigma(r_{i-1},r_i)\right)^2\right\}$ with $a=\ln 10/10$.

This formulation allows for mathematical analysis as summarized next.

Theorem 7 *If* $\sigma(r_{i-1},r_i) < \frac{1}{a}\sqrt{\ln(n_{PL}+1)}$, $\overline{\Gamma}(r_{i-1},r_i) \geq 10\log_{10}\left(\frac{n_{PL}+1}{n_{PL}}\frac{(M_s-1)N_0}{1.5P_0}\left(\iota(r_{i-1},r_i)\xi(r_{i-1},r_i)-\frac{\xi(r_{i-1},r_i)}{n_{PL}}\right)^{-1}\right)$, *and the shadowing correlation is negligible, then the optimization problem of Equation 18 is concave for a convex workspace.*

See (35) for the proof. Theorem 7 characterizes conditions on the underlying channel parameters under which the overall maximization problem can become concave. Intuitively, the stated conditions are sufficient bounds on the uncertainty, resulted from not knowing the true value of the channel, in order to make the problem concave.

Moreover, if the concavity condition holds, then the optimum solution has the following properties (see (35)):

Theorem 8 *Assume that the concavity condition of Theorem 7 holds. Then the optimal solution of Equation 18 satisfies the following properties:*

1. *if* $K_{dB,i-i,i} > K_{dB,j-1,j}$ *and* $\sigma(r_{i-1},r_i)=\sigma(r_{j-1},r_j)$, *then* $d^*_{i-1,i} > d^*_{j-1,j}$,
2. *if* $K_{dB,i-i,i} = K_{dB,j-1,j}$, $\overline{\Gamma}(r_{i-1},r_i) \geq 10\log_{10}\left(\frac{(M_s-1)N_0\left(\exp\{1.5\exp\{(a\sigma(r_{i-1},r_i))^2\}-0.5\}-1\right)}{1.5P_0\xi(r_{i-1},r_i)}\right)$, $\overline{\Gamma}(r_{j-1},r_j) \geq 10\log_{10}\left(\frac{(M_s-1)N_0\left(\exp\{1.5\exp\{(a\sigma(r_{j-1},r_j))^2\}-0.5\}-1\right)}{1.5P_0\xi(r_{j-1},r_j)}\right)$ *and* $\sigma(r_{i-1},r_i) > \sigma(r_{j-1},r_j)$, *then* $d^*_{i-1,i} < d^*_{j-1,j}$,
3. *if* $K_{dB,i-i,i} = K_{dB,j-1,j}$ *and* $\sigma(r_{i-1},r_i)=\sigma(r_{j-1},r_j)$, *then* $d^*_{i-1,i} = d^*_{j-1,j}$,

where $d^*_{i-1,i}$ *is the optimal distance between robots* $i-1$ *and* i.

Theorem 8 methodically compares the length of two route chains as a function of the experienced underlying channel parameters. Intuitively, it shows that as the predicted mean of the channel becomes smaller (indicating a lower channel quality) or there is more uncertainty in channel prediction (higher predicted channel variance), two consecutive robots should

get closer to each other in the corresponding chain. Such mathematical characterizations can be valuable in designing robotic routers in realistic environments.

Figure 10 shows the performance of the optimization problem of Equation 18 as well as the graph-theoretic approach of Equation 16 in a realistic communication environment. We can see that incorporating realistic channel modeling and estimation has a significant impact on the performance. See (35) for more details on the experimental results.

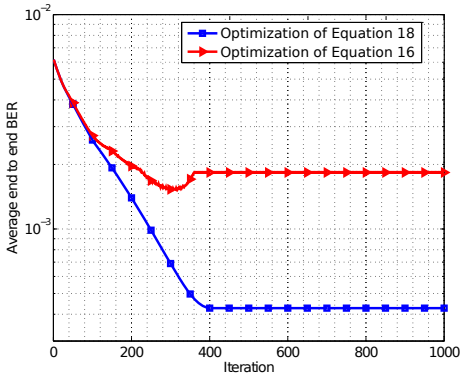

Figure 10: Robotic router optimization – Comparison of the graph-theoretic approach (Equation 16) with a channel-aware approach (Equation 18) in a realistic communication environment. Figure adapted from (35).

6. OTHER CONSIDERATIONS IN COMMUNICATION-AWARE ROBOTICS

- **Co-optimization of communication and motion:** Co-optimization of communication and motion decisions results in interesting interplays between communication and motion parameters such as way-points, motion speed, transmission rate and transmission power. In (65), the motion speed and transmission rate are jointly co-optimized for a robot traveling along a pre-defined path, while (66) jointly designs the path/speed and the transmission rate/power along the path, using an optimal control framework.
- **Co-optimization of communication and sensing:** Explicitly considering sensing objectives and co-optimizing them with motion and communication has also been considered in a number of recent work. For instance, (5) designs the path of an information gathering aerial vehicle by jointly optimizing its sensing and communication while in (6), teams of autonomous underwater vehicles plan their paths to collect informative samples while also optimizing information exchange. In (8, 12), the sensing and communication objectives are explicitly co-optimized for networked robotic target tracking and surveillance.
- **Distributed task servicing:** In (20–23), the robots decide how to efficiently allocate and service tasks among themselves, in a distributed fashion, while being aware of communication considerations. For example, in (22), the robots execute tasks while maintaining desirable communication rates amongst themselves, and in (21), robots maintain connectivity while carrying out their tasks using under-utilized robots as relays.

- **Data gathering and muling:** In (48, 54) robotic data mules plan their trajectories to gather data from stationary sensing nodes, assuming a disk model of connectivity. In (51), an unmanned aircraft ferries data between two stationary nodes on a periodic trajectory, and adaptively allocates the bandwidth along its trajectory to optimize the amount of transferred data.
- **Search and surveillance:** The area of multiple robots searching an area, while maintaining a connected network to effectively cooperate, has also been of interest. References (10, 11) maintain connectivity throughout the duration of the mission while in (7) only periodic connectivity is maintained. Reference (8) considers realistic channel environments and plans search trajectories for optimizing the detection while co-optimizing for communication with the remote station.

SUMMARY POINTS

In this review, we provided an overview of communication-aware robotics, with an emphasis on theoretical characterization and understanding optimality guarantees. Here is a summary of key points.

1. Instead of using over-simplified disk models, robots can use realistic channel models considering the three major dynamics of path loss, shadowing, and multipath and probabilistically predict the channel at unvisited locations, for the purpose of path planning. We then discussed a few theoretical results on different aspects of motion and communication co-optimization, building on this probabilistic framework, as we summarize next.
2. An initially-disconnected unmanned vehicle traveling along a pre-defined path can mathematically characterize the statistics of its traveled distance until connectivity (First Passage Distance), drawing from the literature on Gauss-Markov process. It can further optimize its path in order to reach a guaranteed connected spot with minimum energy consumption. For the latter, we saw that the robot can achieve an asymptotic ϵ-suboptimal solution to this optimization problem using a game theoretic framework.
3. We reviewed results on how multiple robots can optimize their locations/paths in order to cooperatively enable and optimize connectivity/flow of information. In particular, we considered robotic beamformers and robotic routers and discussed properties of the co-optimal communication-motion decisions.

FUTURE ISSUES

Co-optimization of communication and motion and the corresponding use of motion to ensure robust connectivity is a fairly new research area, especially when it comes to theoretical understanding and optimality guarantees. Some possible future directions are as follows.

1. The current state-of-the-art in robotic channel prediction is the probabilistic channel modeling described in this review. There may be other ways to achieve a better channel prediction or to reduce the variance of the predicted model as part of future work.

2. A team of unmanned vehicles can in principle form any network formation that achieves any prescribed level of connectivity and information flow. However, more work is needed in this area to formally solve this problem, in terms of co-optimal motion and communication decisions.
3. Explicitly considering sensing goals in networked robotic operations is another line of future work. For instance, there is room for a more fundamental understanding of the co-optimal sensing, communication, and motion decisions in such networks. Devising algorithms that are independent of the specifics of a particular networked sensing operation can also be very beneficial.
4. Different aspects of communication-aware robotics have been considered and solved in different mathematical frameworks. A unifying approach to this area can be very useful and is a possible future direction.

DISCLOSURE STATEMENT

The authors are not aware of any affiliations, memberships, funding, or financial holdings that might be perceived as affecting the objectivity of this review.

ACKNOWLEDGMENTS

This work was supported by NSF RI award 1619376.

LITERATURE CITED

1. Fukuda T, Nakagawa S. 1987. *A dynamically reconfigurable robotic system (concept of a system and optimal configurations)*. In *IECON'87: Industrial Applications of Robotics & Machine Vision*, vol. 856, pp. 588–595. International Society for Optics and Photonics
2. Kantaros Y, Zavlanos MM. 2016. Distributed communication-aware coverage control by mobile sensor networks. *Automatica* 63:209–220
3. Daniel K, Rohde S, Goddemeier N, Wietfeld C. 2010. *A communication aware steering strategy avoiding self-separation of flying robot swarms*. In *Intelligent Systems (IS), IEEE International Conference*, pp. 254–259
4. Ghaffarkhah A, Mostofi Y. 2014. Dynamic networked coverage of time-varying environments in the presence of fading communication channels. *ACM Transactions on Sensor Networks (TOSN)* 10:45
5. Stachura M, Frew E. 2017. Communication-aware information-gathering experiments with an unmanned aircraft system. *Journal of Field Robotics* 34:736–756
6. Kemna S, Caron DA, Sukhatme GS. 2016. *Adaptive informative sampling with autonomous underwater vehicles: Acoustic versus surface communications*. In *MTS/IEEE OCEANS*, pp. 1–8
7. Hollinger GA, Singh S. 2012. Multirobot coordination with periodic connectivity: Theory and experiments. *IEEE Transactions on Robotics* 28:967–973
8. Ghaffarkhah A, Mostofi Y. 2012. Path planning for networked robotic surveillance. *IEEE Transactions on Signal Processing* 60:3560–3575
9. Stachura M, Frew EW. 2011. Cooperative target localization with a communication-aware unmanned aircraft system. *AIAA Journal of Guidance, Control, and Dynamics* 34:1352–1362
10. Bethke B, How J, Vian J. 2009. *Multi-UAV persistent surveillance with communication con-*

straints and health management. In *Proceedings of the AIAA Guidance, Navigation, and Control Conference*

11. Beard RW, McLain TW. 2003. *Multiple UAV cooperative search under collision avoidance and limited range communication constraints*. In *42nd IEEE International Conference on Decision and Control (IEEE Cat. No. 03CH37475)*, vol. 1, pp. 25–30. IEEE
12. Ghaffarkhah A, Mostofi Y. 2011. Communication-aware motion planning in mobile networks. *IEEE Transactions on Automatic Control* 56:2478–2485
13. Zavlanos MM, Egerstedt MB, Pappas GJ. 2011. Graph-theoretic connectivity control of mobile robot networks. *Proceedings of the IEEE* 99:1525–1540
14. Zavlanos MM, Pappas GJ. 2008. Distributed connectivity control of mobile networks. *IEEE Transactions on Robotics* 24:1416–1428
15. Esposito JM, Dunbar TW. 2006. *Maintaining wireless connectivity constraints for swarms in the presence of obstacles*. In *Proceedings of the IEEE International Conference on Robotics and Automation*
16. Ren W, Beard RW. 2005. Consensus seeking in multiagent systems under dynamically changing interaction topologies. *IEEE Transactions on automatic control* 50:655–661
17. Goddemeier N, Behnke D, Wietfeld C. 2013. *Impact of communication constraints on consensus finding in multi-agent systems*. In *2013 IEEE 24th Annual International Symposium on Personal, Indoor, and Mobile Radio Communications (PIMRC)*, pp. 2464–2468. IEEE
18. Paull L, Huang G, Seto M, Leonard JJ. 2015. *Communication-constrained multi-AUV cooperative SLAM*. In *Proceedings of the IEEE International Conference on Robotics and Automation*
19. Giamou M, Khosoussi K, How JP. 2018. *Talk resource-efficiently to me: Optimal communication planning for distributed loop closure detection*. In *Proceedings of the IEEE International Conference on Robotics and Automation*
20. Ponda S, Redding J, Choi HL, How JP, Vavrina M, Vian J. 2010. *Decentralized planning for complex missions with dynamic communication constraints*. In *American Control Conference (ACC), 2010*, pp. 3998–4003. IEEE
21. Ponda SS, Johnson LB, Kopeikin AN, Choi HL, How JP. 2012. Distributed planning strategies to ensure network connectivity for dynamic heterogeneous teams. *IEEE Journal on Selected Areas in Communications* 30:861–869
22. Zavlanos MM, Ribeiro A, Pappas GJ. 2012. Network integrity in mobile robotic networks. *IEEE Transactions on Automatic Control* 58:3–18
23. Kantaros Y, Zavlanos MM. 2016. Global planning for multi-robot communication networks in complex environments. *IEEE Transactions on Robotics* 32:1045–1061
24. Das SM, Hu YC, Lee CSG, Lu YH. 2007. Mobility-aware ad hoc routing protocols for networking mobile robot teams. *Journal of communications and networks* 9:296–311
25. Dantu K, Sukhatme GS. 2009. *Connectivity vs. control: Using directional and positional cues to stabilize routing in robot networks*. In *Proceedings of the International Conference on Robot Communication and Coordination*
26. Lindhé M, Johansson K. 2009. Using robot mobility to exploit multipath fading. *IEEE Wireless Communications,* 16:30–37
27. Zeng Y, Zhang R. 2017. Energy-efficient uav communication with trajectory optimization. *IEEE Transactions on Wireless Communications* 16:3747–3760
28. Muralidharan A, Mostofi Y. 2020. Statistics of the distance traveled until successful connectivity for unmanned vehicles. *Autonomous Robots, special issue on Robot Communication Challenges* 44:25–42
29. Jiang F, Swindlehurst AL. 2012. Optimization of uav heading for the ground-to-air uplink. *IEEE Journal on Selected Areas in Communications* 30:993–1005
30. Muralidharan A, Mostofi Y. 2017. *Path Planning for a Connectivity Seeking Robot*. In *IEEE Globecom Workshop on Wireless Networking for Unmanned Autonomous Vehicles*, pp. 1–6
31. Muralidharan A, Mostofi Y. 2019. Path planning for minimizing the expected cost until success.

IEEE Transactions on Robotics 35:466–481
32. Muralidharan A, Mostofi Y. 2017. *First Passage Distance to Connectivity for Mobile Robots.* In *American Control Conference (ACC)*, pp. 1517–1523
33. Stump E, Jadbabaie A, Kumar V. 2008. *Connectivity management in mobile robot teams.* In *IEEE International Conference on Robotics and Automation*, pp. 1525–1530
34. Dixon C, Frew E. 2012. Optimizing cascaded chains of unmanned aircraft acting as communication relays. *IEEE Journal on Selected Areas in Communications* 30:883–898
35. Yan Y, Mostofi Y. 2012. Robotic router formation in realistic communication environments. *IEEE Transactions on Robotics,* 28:810–827
36. Chatzipanagiotis N, Zavlanos MM. 2016. Distributed scheduling of network connectivity using mobile access point robots. *IEEE Transactions on Robotics* 32:1333–1346
37. Zeng Y, Zhang R, Lim TJ. 2016. Throughput maximization for uav-enabled mobile relaying systems. *IEEE Transactions on Communications* 64:4983–4996
38. Fink J, Ribeiro A, Kumar V. 2013. Robust control of mobility and communications in autonomous robot teams. *IEEE Access* 1:290–309
39. Kim Y, Mesbahi M. 2005. *On maximizing the second smallest eigenvalue of a state-dependent graph Laplacian.* In *American Control Conference (ACC),*, pp. 99–103. IEEE
40. Zhan P, Yu K, Swindlehurst AL. 2011. Wireless relay communications with unmanned aerial vehicles: Performance and optimization. *IEEE Transactions on Aerospace and Electronic Systems* 47:2068–2085
41. Schouwenaars T, Stubbs A, Paduano J, Feron E. 2006. Multivehicle path planning for nonline-of-sight communication. *Journal of Field Robotics* 23:269–290
42. Chatzipanagiotis N, Liu Y, Petropulu A, Zavlanos M. 2012. *Controlling groups of mobile beamformers.* In *IEEE Conference on Decision and Control (CDC)*, pp. 1984–1989
43. Kalogerias DS, Petropulu AP. 2016. *Mobile beamforming & spatially controlled relay communications.* In *IEEE International Conference on Acoustics, Speech and Signal Processing (ICASSP)*, pp. 6405–6409
44. Kalogerias DS, Petropulu AP. 2018. Spatially controlled relay beamforming. *IEEE Transactions on Signal Processing* 66:6418–6433
45. Muralidharan A, Mostofi Y. 2017. Energy optimal distributed beamforming using unmanned vehicles. *IEEE Transactions on Control of Network Systems*
46. Muralidharan A, Mostofi Y. 2016. *Distributed beamforming using mobile robots.* In *IEEE International Conference on Acoustics, Speech and Signal Processing (ICASSP)*, pp. 6385–6389
47. Yan Y, Mostofi Y. 2016. Efficient clustering and path planning strategies for robotic data collection using space-filling curves. *IEEE Transactions on Control of Network Systems*
48. Tekdas O, Isler V, Lim JH, Terzis A. 2009. Using mobile robots to harvest data from sensor fields. *IEEE Wireless Communications* 16:22–28
49. Hollinger G, Choudhary S, Qarabaqi P, Murphy C, Mitra U, et al. 2012. Underwater data collection using robotic sensor networks. *IEEE Journal on Selected Areas in Communications* 30:899–911
50. Yan Y, Mostofi Y. 2014. To go or not to go: On energy-aware and communication-aware robotic operation. *IEEE Transactions on Control of Network Systems,* 1:218–231
51. Carfang AJ, Frew EW, Kingston DB. 2014. Cascaded optimization of aircraft trajectories for persistent data ferrying. *AIAA Journal of Aerospace Information Systems* 11:807–820
52. Say S, Inata H, Liu J, Shimamoto S. 2016. Priority-based data gathering framework in uav-assisted wireless sensor networks. *IEEE Sensors Journal* 16:5785–5794
53. Sugihara R, Gupta RK. 2011. Path planning of data mules in sensor networks. *ACM Transactions on Sensor Networks (TOSN)* 8:1–27
54. Bhadauria D, Tekdas O, Isler V. 2011. Robotic data mules for collecting data over sparse sensor fields. *Journal of Field Robotics* 28:388–404
55. Mozaffari M, Saad W, Bennis M, Debbah M. 2017. Wireless communication using unmanned

aerial vehicles (uavs): Optimal transport theory for hover time optimization. *IEEE Transactions on Wireless Communications* 16:8052–8066

56. Alzenad M, El-Keyi A, Yanikomeroglu H. 2017. 3d placement of an unmanned aerial vehicle base station for maximum coverage of users with different qos requirements. *IEEE Wireless Communications Letters*
57. Ghaffarkhah A, Mostofi Y. 2010. *Channel learning and communication-aware motion planning in mobile networks*. In *American Control Conference (ACC),*, pp. 5413–5420. IEEE
58. Malmirchegini M, Mostofi Y. 2012. On the spatial predictability of communication channels. *IEEE Transactions on Wireless Communications,* 11:964–978
59. Caccamo S, Parasuraman R, Freda L, Gianni M, Ogren P. 2017. *RCAMP: Resilient Communication-Aware Motion Planner and Autonomous Repair of Wireless Connectivity in Mobile Robots*. In *IEEE/RSJ International Conference on Intelligent Robots and Systems (IROS)*, pp. 2153–0866
60. Carfang AJ, Wagle N, Frew EW. 2015. Integrating nonparametric learning with path planning for data-ferry communications. *Journal of Aerospace Information Systems* 12:784–799
61. Kalogerias DS, Petropulu AP. 2015. *Nonlinear spatiotemporal channel gain map tracking in mobile cooperative networks*. In *Proceedings of the IEEE International Workshop on Signal Processing Advances in Wireless Communications*
62. Parasuraman R, Oegren P, Min BC. 2018. *Kalman filter based spatial prediction of wireless connectivity for autonomous robots and connected vehicles*. In *Proceedings of the IEEE Vehicular Technology Conference*
63. Narayanan VK, Miyashita T, Horikawa Y, Hagita N. 2018. *A transient-goal driven communication-aware navigation strategy for large human-populated environments*. In *Proceedings of the IEEE/RSJ International Conference on Intelligent Robots and Systems*
64. Nurellari E, Licea DB, Ghogho M. 2019. *Optimum Trajectory Planning for Robotic Data Ferries in Delay Tolerant Wireless Sensor Networks*. In *Proceedings of the European Signal Processing Conference*
65. Yan Y, Mostofi Y. 2013. Co-optimization of communication and motion planning of a robotic operation under resource constraints and in fading environments. *IEEE Transactions on Wireless Communications,* 12:1562–1572
66. Ali U, Cai H, Mostofi Y, Wardi Y. 2018. Motion-communication co-optimization with cooperative load transfer in mobile robotics: an optimal control perspective. *IEEE Transactions on Control of Network Systems*
67. Cai H, Mostofi Y. 2019. Human-robot collaborative site inspection under resource constraints. *IEEE Transactions on Robotics* 35:200–215
68. Rappaport TS. 1996. *Wireless communications: principles and practice*, vol. 2. prentice hall PTR New Jersey
69. Hashemi H. 1994. *A study of temporal and spatial variations of the indoor radio propagation channel*. In *IEEE International Symposium on Personal, Indoor and Mobile Radio Communications*, pp. 127–134. IEEE
70. Siegert AJ. 1951. On the first passage time probability problem. *Physical Review* 81:617
71. Dudley RM. 2002. *Real analysis and probability*, vol. 74. Cambridge University Press
72. Papoulis A, Pillai SU. 2002. *Probability, random variables, and stochastic processes*. Tata McGraw-Hill Education
73. Mehr C, McFadden J. 1965. Certain properties of gaussian processes and their first-passage times. *Journal of the Royal Statistical Society. Series B (Methodological)* :505–522
74. Ricciardi LM, Sato S. 1988. First-passage-time density and moments of the ornstein-uhlenbeck process. *Journal of Applied Probability* :43–57
75. Di Nardo E, Nobile A, Pirozzi E, Ricciardi L. 2001. A computational approach to first-passage-time problems for gauss–markov processes. *Advances in Applied Probability* 33:453–482
76. Cover TM, Thomas JA. 2012. *Elements of information theory*. John Wiley & Sons

77. Robert CP. 1996. Intrinsic losses. *Theory and decision* 40:191–214
78. Smith W, Cox D. 2004. Urban propagation modeling for wireless systems. Tech. rep., DTIC Document
79. Fudenberg D, Tirole J. 1991. Game theory, 1991. *Cambridge, Massachusetts* 393:12
80. Monderer D, Shapley L. 1996. Potential games. *Games and economic behavior* 14:124–143
81. Marden JR, Shamma JS. 2012. Revisiting log-linear learning: Asynchrony, completeness and payoff-based implementation. *Games and Economic Behavior* 75:788–808
82. Tse D, Viswanath P. 2005. *Fundamentals of wireless communication*. Cambridge university press
83. Mudumbai R, Brown III D, Madhow U, Poor H. 2009. Distributed transmit beamforming: challenges and recent progress. *IEEE Communications Magazine,* 47:102–110
84. Ochiai H.and Mitran P, Poor H, Tarokh V. 2005. Collaborative beamforming for distributed wireless ad hoc sensor networks. *IEEE Transactions on Signal Processing,* 53:4110–4124
85. Karanam CR, Korany B, Mostofi Y. 2018. *Magnitude-based angle-of-arrival estimation, localization, and target tracking*. In *2018 17th ACM/IEEE International Conference on Information Processing in Sensor Networks (IPSN)*, pp. 254–265. IEEE
86. De Gennaro MC, Jadbabaie A. 2006. *Decentralized control of connectivity for multi-agent systems*. In *45th IEEE Conference on Decision and Control*, pp. 3628–3633. IEEE
87. Dai R, Maximoff J, Mesbahi M. 2013. Optimal trajectory generation for establishing connectivity in proximity networks. *IEEE Transactions on Aerospace and Electronic Systems* 49:1968–1981